J. Phys. B: At. Mol. Opt. Phys. 27 (1994) 4057–4072. Printed in the UK

Differential cross sections for the electron impact excitation of the a $^1\Delta_g$ and b $^1\Sigma_g^+$ electronic states of O_2

A G Middleton†, M J Brunger†, P J O Teubner†, M W B Anderson†, C J Noble‡, G Wöste§, K Blum§, P G Burke‖ and C Fullerton‖

† Institute of Atomic Studies, School of Physical Sciences, The Flinders University of South Australia, Bedford Park, SA 5042, Australia

‡ DRAL Daresbury Laboratory, Warrington, WA4 4AD, UK

§ Institut für Theoretische Physik I, Westfälische Wilhelms Universität, Münster, Germany

‖ Queen's University of Belfast, Belfast BT7 1NN, UK

Received 19 August 1993, in final form 10 June 1994

Abstract. Experimental and theoretical differential cross sections for the electron impact excitation of the a $^1\Delta_g$ and b $^1\Sigma_g^+$ electronic states of O_2 have been determined at ten incident energies ranging from 5 eV to 20 eV. The current experimental differential cross sections were obtained for the scattering range 10° to 90° by analysing energy loss spectra in O_2 at a number of fixed scattering angles within that range. This data represents an extension to and comprehensive remeasurement of the pioneering work of Trajmar and co-workers for this scattering system. The present theoretical results were obtained using the *R*-matrix method with a model including nine electronic states of the target molecule and configuration interaction (CI) representations of the target wavefunctions. It represents one of the first *ab initio* calculations of electron scattering from an open-shell molecule.

1. Introduction

Detailed information about collisions between low-energy electrons and oxygen molecules is required in understanding the physics of planetary atmospheres, gaseous discharges and both astrophysical and laboratory plasmas. In particular, transitions to the lowest-lying excited electronic states (a $^1\Delta_g$, b $^1\Sigma_g^+$) from the ground molecular state (X $^3\Sigma_g^-$) give rise to the atmospheric infrared (Herzberg) and red (Babcock) bands, respectively. The metastable a $^1\Delta_g$ state is also important in the operation of the O_2–I_2 mixing laser (McDermott *et al* 1978) and further, because its lifetime is of the order of 2700 s (Badger *et al* 1965), it permits the production of an adequate number density to enable the study of scattering from an excited molecular species by means of a collision experiment (Khakoo *et al* 1983).

We have previously discussed the earlier experimental and theoretical studies on electron impact excitation of the a $^1\Delta_g$ and b $^1\Sigma_g^+$ states in Noble and Burke (1992) and Middleton *et al* (1992). These two letters concentrated on integral cross sections for the excitation of the a and b channels and in particular looked at the mechanism for the resonance enhancement observed in the a and b integral cross sections that was found in both these studies. Consequently we do not review the earlier work in detail here but simply provide a short resumé of it.

0953-4075/94/174057+16$19.50

Experimental investigations into electron impact excitation of the a $^1\Delta_g$ and b $^1\Sigma_g^+$ states have been limited. Schulz and Dowell (1962) reported upper limits on the integral cross sections for near threshold excitation of the a $^1\Delta_g$ and b $^1\Sigma_g^+$ states of 3×10^{-20} cm^2 and 6×10^{-21} cm^2, respectively, using the trapped electron method. Skerbele *et al* (1968) found that the relative intensities of the a $^1\Delta_g$ state referred to the elastic peak remained constant in the scattering range 3° to 12° for electrons whose incident energy was 45 eV. Konishi *et al* (1970) reported integral cross sections for collision energies in the range 20–70 eV while Linder and Schmidt (1971) detailed differential and integral cross sections for elastic scattering, vibrational excitations ($v' = 1$–4) of the ground electronic state, and electronic excitation of the a $^1\Delta_g$ and b $^1\Sigma_g^+$ states with electrons of incident energies in the range from threshold to 4 eV. At about the same time Trajmar *et al* (1971) measured differential and integral cross sections, in the energy range 4–45 eV, for excitation of the a $^1\Delta_g$ and b $^1\Sigma_g^+$ electronic states. The differential cross sections were measured with a crossed beam configuration over the scattered angular range 10°–90°. Absolute values were then assigned by applying a novel deconvolution procedure to the measured energy loss spectra and assuming a knowledge of the absolute elastic differential cross section.

Wong *et al* (1973) measured differential cross sections for the a $^1\Delta_g$ and b $^1\Sigma_g^+$ electronic states at an electron scattering angle of 25° and incident beam energies in the regime 4–15 eV. Subsequent to this Wakiya (1978a, b) reported both differential and integral cross sections for the a $^1\Delta_g$ and b $^1\Sigma_g^+$ states for energies in the range 20–200 eV and at scattering angles from 10°–130°. The hitherto most recent experimental investigation into the electron impact excitation of the a $^1\Delta_g$ and b $^1\Sigma_g^+$ states was made by Shyn and Sweeney (1993) who reported both differential and integral cross sections. In this study the impact energy ranged from 5–20 eV while the scattering angle range was 12°–156°. However, similar to Trajmar *et al* (1971) this work did not investigate the influence of the $^2\Pi_u$ resonance on the differential cross sections.

Until recently there had been very little theoretical interest in calculating excitation cross sections for the a $^1\Delta_g$ and b $^1\Sigma_g^+$ states of O_2 with, for many years, the only study available being the semi-empirical estimates of Watson *et al* (1967). However, Noble and Burke (1986, 1992) have applied their *R*-matrix method to report integral cross sections for excitation of both the a and b states while Gauyacq *et al* (1987) have employed a multichannel effective range approach to calculating integral cross sections for these same states from threshold to 12 eV. Detailed comparisons between theory and experiment at the integral cross section level can be found in both Noble and Burke (1992) and Middleton *et al* (1992).

It is the purpose of this paper to report new experimental and theoretical cross sections for electron impact excitation of the a $^1\Delta_g$, and b $^1\Sigma_g^+$ states. In section 2 we describe the experimental apparatus and method used in the current measurements whilst in section 3 details of the calculation are provided. Finally, a comprehensive comparison between the present theoretical and experimental results, and with the earlier data, is made in section 4.

2. Experimental apparatus and method

The present measurements have been carried out with the aid of a high resolution electron monochromator. A detailed description of the apparatus, which is schematically presented in figure 1, and its principles of operation were given previously by

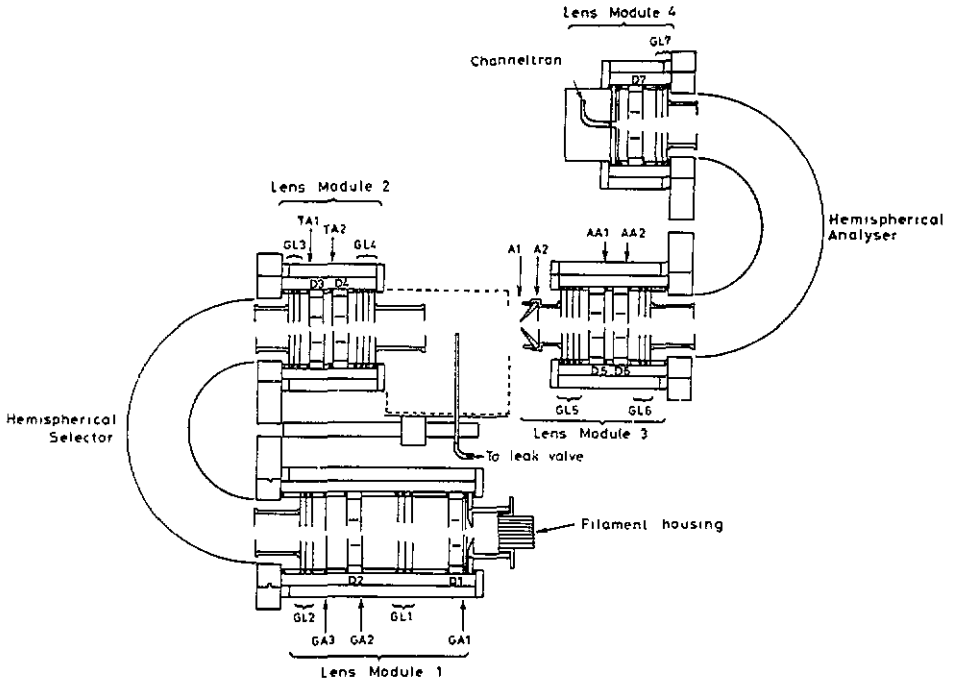

Figure 1. Schematic diagram of the electron monochromator.

Brunger and Teubner (1990). Briefly, a beam of O_2 effusing from a molybdenum tube of internal diameter 0.6 mm is crossed with a beam of electrons of desired energy E_0. Elastically and inelastically scattered electrons at a particular scattering angle (θ) are energy analysed and detected. Allowance was made for the background contribution arising from both primary electron beam interference and stray electrons entering the detector. For scattering angles $\theta > 20°$ these sources of background were very small. The background contribution was determined by comparison of the scattered signal with the molecular beam on and off. The overall energy resolution of the monochromator for these experiments was ~65 meV (FWHM) and, under normal operating conditions, incident electron beam currents of about 1 nA were obtained in the interaction region for the energy regime of the present study. The angular resolution, from geometric and electron optic considerations, is estimated to be 1°.

At each incident energy, energy-loss spectra were recorded at each scattering angle over the energy-loss range −0.2 eV to +2.3 eV. A typical spectrum is shown in figure 2. The spectra were obtained by ramping the analyser in the energy loss mode in conjunction with a multichannel scaler which stored the scattered signal as a function of energy loss. The data was then transferred to a mainframe computer for analysis. Each spectrum was analysed via a computer least-squares fitting technique which was thoroughly discussed previously by Brunger and Teubner (1990). Briefly, however, the general form of the fitting function is given by:

$$S(E_0, \theta, W, \rho, I_0) = \sum_{n'=0}^{N} X_{n'}(E_0, \theta) \sum_{v'=0}^{M(n')} q_{v'v''} \times F(W_{n'v'} - W) + B(E_0, \theta, W, \rho, I_0) \qquad (1)$$

where $S(E_0, \theta, W, \rho, I_0)$ is the signal as measured by the experimental apparatus, $X_{n'}$ is proportional to the differential cross section for the electronic state n', $q_{v'v''}$ is the

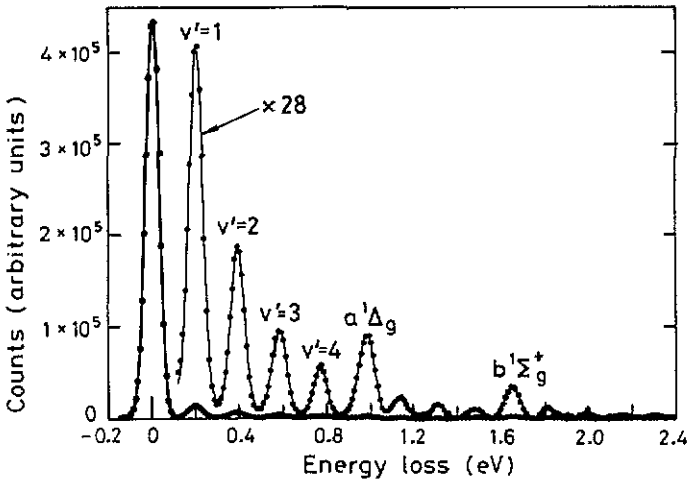

Figure 2. Energy loss spectrum in O_2. The electron scattering angle was 60° and the incident electron energy was 11 eV. The present data (●) and the deconvoluted fit to this data (——) are shown. For clarity the inelastic data, scaled by a factor of 28, are also shown.

Franck–Condon factor, B represents any background contribution to the measured signal, W is the energy loss. $W_{n'v'}$ is the energy of each vibrational sub-level relative to the $v''=0$ vibrational sub-level of the $X\,^3\Sigma_g^-$ ground-electronic state and $F(W_{n'v'}-W)$ is a function which characterized the experimental resolution of the analyser.

The experimental resolution, $F(W_{n'v'}-W)$, was shown to be Gaussian in form so that,

$$F(X)=\frac{1}{\Delta\sqrt{2\pi}}\exp\left(-\frac{X^2}{2\Delta^2}\right) \tag{2}$$

where Δ is related to the full width at half maximum (FWHM) energy resolution and is a parameter to be determined in the fit. We note that in the present study the energy of each vibrational sub-level relative to the $v''=0$ vibrational sub-level of the $X\,^3\Sigma_g^-$ ground electronic state and the corresponding Franck–Condon factor were obtained from Trajmar *et al* (1971).

The quantities $X_{n'}(E_0, \theta)$, B and Δ are determined, for a given energy-loss spectrum, from equations (1) and (2) by requiring the difference between the calculated and measured spectrum be a minimum in a least squares sense (Cartwright *et al* 1977). An example of a fit to the data is shown as a line in figure 2.

The fitting procedure thus yielded the ratio of the differential cross section for the inelastic feature of interest $\sigma_{n'}(E_0, \theta)$, to the elastic differential cross section $\sigma_0(E_0, \theta)$. That is:

$$R_{n'}(E_0, \theta)=\frac{X_{n'}(E_0, \theta)}{X_0(E_0, \theta)}=\frac{\sigma_{n'}(E_0, \theta)}{\sigma_0(E_0, \theta)}. \tag{3}$$

It is immediately apparent from equation (3) that the product $R\sigma_0(E_0, \theta)$ then gives the required electronic state differential cross section provided $\sigma_0(E_0, \theta)$ is known.

An important aspect of energy loss measurements obtained in this fashion is to have a knowledge of the transmission of the scattered electron analyser. This is especially true when the residual energy of the scattered electron is small as it is in this regime

that the detector electron optics can become severely chromatic. In addition, low energy electrons are very sensitive to stray electric and magnetic fields as well as to surface conditions. Thus the transmission efficiency of the analyser can vary quite radically for near-zero residual energies.

The technique we employed to calibrate the transmission of the analyser was first explored by Pichou *et al* (1976) and was discussed previously by Brunger *et al* (1989). In essence, however, it relies on the fact that the yield of ejected electrons from helium following near threshold ionization is constant and thus any deviations from flatness directly reflects the distortion introduced by the non-uniform transmission efficiency of the analyser. A typical example of the present analyser response can be found in figure 2 of Brunger and Teubner (1990), which demonstrated that the transmission of the scattered electrons was constant to better than 5% over a wide range of residual electron energies. This result is a reflection of the excellent lensing performance of the first post-collision zoom lens of the analyser electron optics.

In a separate series of experiments we have measured elastic angular distributions for each E_0 studied. Details of the procedure for these experiments can also be found in Brunger *et al* (1989). Where possible the present elastic data were placed on an absolute scale by normalizing to the relevant tabulated data of Shyn and Sharp (1982), typically at the scattering angle of 50°. However, at some of the energies of the present study Shyn and Sharp did not provide elastic differential cross sections and on these occasions we interpolated their data and then used the appropriate value derived from this interpolation to normalize our data. We note that in the energy regime of the present study this is a valid procedure as resonance enhancement in the elastic channel is small (Noble and Burke 1992). We do not tabulate the present elastic data here but it was found that the present data were in better agreement at foward and middle angles with the elastic differential cross sections of Shyn and Sharp than those of Trajmar *et al* (1971). This point is illustrated in figures 3(*a*) and 3(*b*) where we compare the present elastic differential cross sections with the earlier data for electrons of incident energies 7 eV and 20 eV, respectively. Furthermore, we have specifically checked the absolute value of the O_2 elastic differential cross sections at $E_0 = 10$ eV and $\theta = 30°$ by running consecutive experiments in O_2 and He under identical electron-optical conditions and carefully controlled gas-pressure conditions. The relative gas densities were obtained by monitoring the background chamber pressure with an ion gauge (GP274013) and applying the manufacturer's ionization calibration factors. The cross section was then placed on an absolute scale by normalizing to the relevant cross section for elastic scattering in helium as calculated by Nesbet (1979). The present value was found to agree with the earlier number of Shyn and Sharp (1982) to better than 5%. Consequently we have chosen the elastic differential cross section data of Shyn and Sharp (1982) to enable us to determine the desired electronic state differential cross sections, $\sigma_{n'}(E_0, \theta)$.

As in previous measurements the zero scattering angle was determined as that about which the elastic scattering intensity was symmetric. The estimated error in this determination is ±1°. The electron energy scale was calibrated against the He 2^2S resonance at 19.367 eV and is estimated to be accurate to better than 50 meV.

3. Details of the calculation

The theoretical results presented here have been calculated using *R*-matrix theory. The underlying theoretical framework has been developed into a now well established and

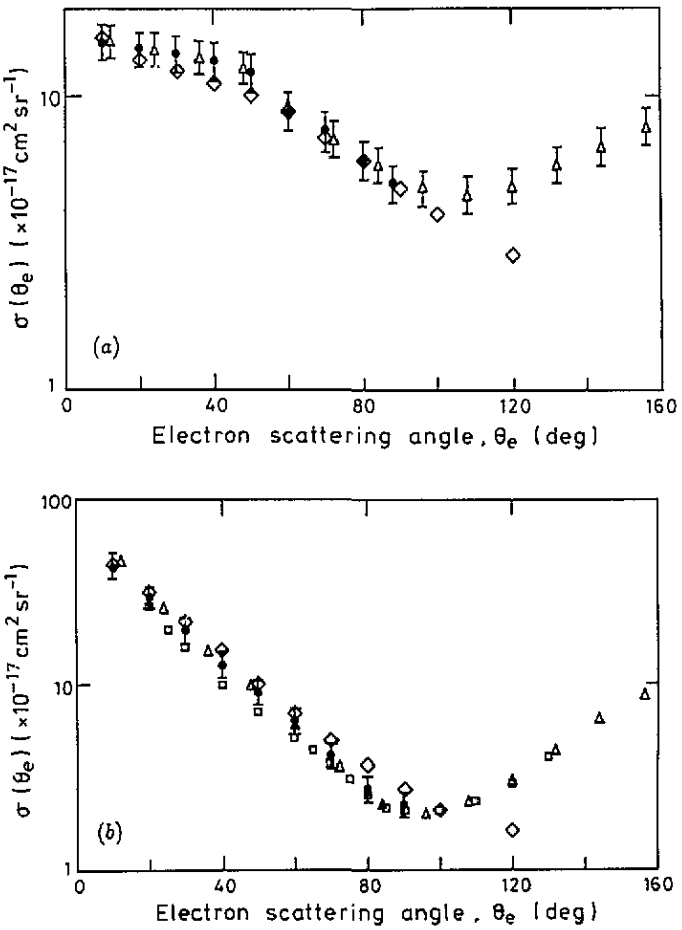

Figure 3. Elastic differential scattering cross sections for O_2. (*a*) $E_0=7$ eV, (*b*) $E_0=20$ eV. The present results (●) are compared with the earlier work of Shyn and Sharp (1982) (△), Trajmar *et al* (1971) (◇) and Wakiya (1978a, b) (□).

successful computational technique for calculating cross sections for collisions between photons, electrons or positrons and diatomic molecules. The detailed computational procedures have been described in a number of reviews (e.g. Gillan *et al* 1987) so only a summary of the main features will be presented here to establish notation and to define the model used in this work.

The fundamental concept underlying *R*-matrix theory is that the solution of the Schrödinger equation may be simplified by dividing the calculation into two or more spatial regions. The description of the collision is then approximated according to the form of the interaction between the projectile and the target within a particular region. In the present calculation configuration space is divided into two regions according to whether or not the incident electron is inside the charge cloud of the target. The inner region is a hypersphere in configuration space defined by the condition $r \leqslant a$ where r is the radial coordinate of the incident electron and a is a constant chosen so that the charge density of the target has effectively vanished by the boundary of the inner region ($a=10.0$ au in the present work). As the inner region is finite, it may be spanned by a denumerable set of discrete basis states and the usual problem of treating continuum

states is avoided. The collision complex in the inner region acts as an excited molecular state and may be treated using modified versions of standard quantum chemistry methods. As a first step the fixed nuclei approximation is invoked. This corresponds to neglecting the nuclear motion and as a consequence all quantities calculated using the approximation depend parametrically on the internuclear separation. The effects of nuclear motion may be reinstated in subsequent stages of the calculation if required.

The Hamiltonian of the scattering system in the inner region is diagonalized using an energy-independent R-matrix basis of the form

$$\Psi_k = \mathscr{A} \sum_{ij} \bar{\Phi}_i(1 \ldots N, \hat{r}_{N+1}\sigma_{N+1}; R)u_j(r_{N+1}; R)c_{ijk} + \sum_q \Phi_q(1 \ldots N+1; R)c_{qk} \qquad (4)$$

to determine the variational coefficients c_{ijk} and c_{qk}. The initial close-coupling summation in equation (4) involves products of channel functions, $\bar{\Phi}_i$, which are constructed from target eigenstates (or pseudo-states) and the spin-angle functions of the scattered electron. The second summation in equation (4) involves $\mathscr{L}^2$-integrable $(N+1)$-electron terms and is constructed to relax orthogonality constraints and to account for short-range polarization effects. The function $u_j(r)$ represent the radial wavefunction of the scattered electron and the operator $\mathscr{A}$ indicates that this electron must by antisymmetrized with respect to the target electrons. The sum over channel functions is chosen to include the nine O_2 electronic states $X\,^3\Sigma_g^-$, $a\,^1\Delta_g$, $b\,^1\Sigma_g^+$, $c\,^1\Sigma_u^-$, $C\,^3\Delta_u$, $A\,^3\Sigma_u^+$, $B\,^3\Sigma_u^-$, $^1\Delta_u$ and $^1\Sigma_u^+$ corresponding to the principal configurations [core] $1\pi_u^4 1\pi_g^2$ and [core] $1\pi_u^3 1\pi_g^3$. Each of these states is represented by a valence configuration interaction (VCI) wavefunction calculated using σ and π SCF orbitals obtained using the Slater basis of Saxon and Liu (1977). The wavefunctions are limited to single and double valence excitations. This includes significant target correlation effects and has been shown by Beebe *et al* (1976) to provide a good representation of the shapes and relative spacing of the potential energy curves. These properties are more important in scattering than reproducing the absolute energies of the states. Details of these target representations are shown in table 1. The relative excitation energy of the lowest three states is

Table 1. Oxygen target configuration interaction wavefunctions used in the R-matrix calculations. Calculated vertical excitation energies (fixed internuclear separation $R = 2.3\ a_0$) compared with values quoted by Teillet-Billy *et al* (1987) (see Krupenie 1972, Huber and Herzberg 1979, Buenker and Peyerimhoff 1975). The number of configuration state functions (CSFs) in each target wavefunction are also shown.

O_2 target state	Calculated excitation energy (eV)	Estimated excitation energy (eV)	Number of CSFs
$X\,^3\Sigma_g^-$	0.00	0.00	17
$a\,^1\Delta_g$	0.93	0.98	13
$b\,^1\Sigma_g^+$	1.47	1.65	19
$c\,^1\Sigma_u^-$	5.49	6.12	14
$C\,^3\Delta_u$	5.68	6.27	16
$A\,^3\Sigma_u^+$	5.81	6.47	18
$B\,^3\Sigma_u^-$	10.86	9.25	20
$^1\Delta_u$	13.16	11.8	14
$^1\Sigma_u^+$	14.67	13.25	16

seen to be accurate to within 0.2 eV. The calculated excitation energies of the three 6 eV states are low with respect to the ground state but their relative separations are within 0.1 eV of the correct values. The optically allowed B state lies 1.6 eV too low

with respect to the ground state. It should be noted, however, that the minima of each of these potential energy curves occur at internuclear separations around 0.5 a_0 larger than the equilibrium value for the ground state so that the curves are rising steeply at the separation considered here (Saxon and Liu 1977).

The continuum orbitals u_j in equation (4) are obtained by numerically solving a single-channel model scattering problem and then Schmidt orthogonalizing the resulting solutions with respect to the bound molecular orbitals to obtain a single orthonormal orbital set in which to perform the scattering calculation. SCF σ_g and σ_u virtual orbitals are included in this set in addition to those occupied in the ground state. Continuum functions complete over the energy range 0–6 Ryd and including partial waves up to $l=5$ for σ, π and δ symmetries are included in the calculations. The resulting Hamiltonian matrices have dimensions of a few hundred and are diagonalized so that the R-matrix can be calculated. The R-matrix is given by

$$R_{ij}=\sum_k \frac{w_{ik}(a)w_{jk}(a)}{E-E_k} \tag{5}$$

where the E_k are R-matrix eigenenergies and the factors $w_{ij}(a)$ reduced width amplitudes. Both of these quantities are obtained from the inner region diagonalization.

In the external region it is assumed that the scattered electron is distinguishable from the target electrons and therefore need not be antisymmetrized with them. Further, the interaction between the target and the scattered electron is represented by a multipolar static interaction including both dipole and quadrupole terms. The R-matrix then provides the boundary conditions for the integration of the coupled Schrödinger equations in the external region resulting from these assumptions. The integration has been carried out using a combination of Light–Walker propagator and accelerated Gailitis asymptotic expansion methods (Burke and Noble 1994).

The asymptotic form of the external region wavefunction allows K-matrices, $\boldsymbol{K}$, to be calculated. Scattering T-matrices, $\boldsymbol{T}$, are then obtained using

$$\boldsymbol{T}=\frac{-2\boldsymbol{K}}{\boldsymbol{I}-\mathrm{i}\boldsymbol{K}}. \tag{6}$$

The T-matrix may be used to calculate the differential cross section according to the expression

$$\left(\frac{\mathrm{d}\sigma}{\mathrm{d}\Omega}\right)_{ij}=\sum_k A_{ij}^k P_k(\cos\theta) \tag{7}$$

where P_k is a Legendre polynomial and θ is the angle between the incident and scattered electron beams. The coefficients A_{ij}^k are given by

$$A_{ij}^k(E)=\frac{(-1)^k\hat{k}}{16\hat{S}E}\sum_{l_il_i'l_jl_j'}\mathrm{i}^{l_i-l_j-l_i'+l_j'}\sqrt{\hat{l}_i\hat{l}_i'\hat{l}_j\hat{l}_j'}\begin{pmatrix}l_i & l_i' & k\\ 0 & 0 & 0\end{pmatrix}\begin{pmatrix}l_j & l_j' & k\\ 0 & 0 & 0\end{pmatrix}$$
$$\times\sum_{j_t}(-1)^{j_t}\hat{j}_t\times\begin{Bmatrix}l_i' & l_i & k\\ l_j & l_j' & j_t\end{Bmatrix}\sum_S \hat{S}\mathscr{T}^{j_tS}_{l_i,l_j}\mathscr{T}^{j_tS*}_{l_i',l_j'} \tag{8}$$

where l_i, l_j are the angular momentum of the incident and scattered electron, respectively and S the spin. In equation (8) we have used the standard notation for 3-j and 6-j symbols and the notation $\hat{m}$ to represent $2m+1$. The differential cross section given by

Table 2. Experimental differential cross sections (10^{-19} cm^2 sr^{-1}) for electron impact excitation of the a $^1\Delta_g$ electronic state.

Scattering angle θ_e (deg)	$\sigma(\theta)$ Incident electron beam energy (eV)									
	5.0	6.0	7.0	8.0	9.0	9.5	10.0	11.0	15.0	20.0
10	6.57	6.99	1.84	0.48	7.01	9.98	18.33	6.14	5.91	2.21
20	7.95	6.23	2.45	3.24	13.61	11.55	13.69	8.57	4.79	2.16
30	7.94	5.36	3.67	8.79	10.90	10.95	11.02	6.99	4.59	1.88
40	7.91	5.30	4.44	6.75	9.61	8.87	10.27	6.43	3.79	1.72
50	6.67	5.50	4.52	6.49	7.86	7.41	9.96	6.41	3.34	1.88
60	5.38	5.92	4.81	5.43	7.58	7.77	10.09	5.98	3.43	2.00
70	5.54	5.78	5.17	6.25	6.93	7.89	8.78	6.18	4.52	1.62
80	5.34	5.26	4.82	6.23	6.87	7.99	8.43	5.83	4.61	1.66
90	5.88	6.10	5.86	6.19	6.35	7.67	7.47	5.52	3.78	2.11

equations (7) and (8) is expressed in terms of the angular momentum transfer, j_t, as suggested by Fano and Dill (1972). The reduced T-matrices, $\mathscr{T}$, are linear combinations of those given by equation (6) (see for example, Dill and Dehmer 1974). The differential cross sections have been evaluated using a program written by Wöste and Fullerton (1994).

4. Results and discussion

The experimental differential cross sections for the electron impact excitation of the a $^1\Delta_g$ and b $^1\Sigma_g^+$ states of O_2 from the ground electronic state are given in tables 2 and 3 respectively. The overall uncertainty in the present data ranged from 17–25% for the excitation of the a $^1\Delta_g$ state and 19–30% for the b $^1\Sigma_g^+$ state excitation. This uncertainty arose by combining in quadrature uncertainty in the normalization procedure (14%) with statistical uncertainties in $R_{n'}(E_0, \theta)$, an uncertainty in our detector response calibration (~10%) and the uncertainty in the fitting procedure as determined by the

Table 3. Experimental differential cross sections (10^{-19}cm^2 sr^{-1}) for electron impact excitation of the b $^1\Sigma_g^+$ electronic state.

Scattering angle θ_e (deg)	$\sigma(\theta)$ Incident electron beam energy (eV)									
	5.0	6.0	7.0	8.0	9.0	9.5	10.0	11.0	15.0	20.0
10	—	0.61	0.62	0.012	0.48	0.53	2.43	0.43	1.20	0.47
20	—	0.80	1.01	0.30	2.02	1.53	3.07	1.62	1.10	0.49
30	—	1.10	1.25	1.43	2.56	2.41	3.11	2.19	1.15	0.59
40	—	0.99	1.61	1.83	3.38	2.95	3.57	2.72	1.27	0.61
50	—	0.65	1.92	2.41	3.64	3.21	3.41	3.30	1.58	0.72
60	—	0.56	1.70	2.18	3.10	3.60	3.48	3.01	1.38	0.62
70	—	0.70	1.59	2.36	3.02	3.10	2.96	2.87	1.35	0.60
80	—	0.89	1.64	2.01	2.52	2.84	2.64	2.37	1.17	0.72
90	—	1.38	1.81	1.94	2.05	2.57	2.67	2.17	1.01	0.77

Table 4. Theoretical differential cross sections (10^{-19}cm^2 sr^{-1}) for electron impact excitation of the a $^1\Delta_g$ electronic state.

Scattering angle θ_e (deg)	$\sigma(\theta)$ Incident electron beam energy (eV)									
	5.0	6.0	7.0	8.0	9.0	9.5	10.0	11.0	15.0	20.0
0	6.47	6.78	8.38	11.52	4.81	4.20	3.86	3.39	3.95	—
7	6.38	6.68	8.25	11.43	4.82	4.21	3.87	3.40	3.85	—
15	6.11	6.39	7.88	11.19	4.84	4.24	3.90	3.43	3.61	—
22	5.74	5.99	7.33	10.83	4.91	4.30	3.96	3.50	3.41	—
30	5.38	5.57	6.70	10.43	5.04	4.43	4.08	3.63	3.41	—
37	5.11	5.22	6.11	10.07	5.26	4.64	4.29	3.85	3.70	—
45	5.02	5.01	5.61	9.80	5.58	4.95	4.59	4.15	4.24	—
52	5.13	4.99	5.30	9.69	6.01	5.36	4.97	4.52	4.87	—
60	5.42	5.15	5.17	9.75	6.53	5.85	5.43	4.94	5.40	—
67	5.81	5.42	5.19	9.96	7.10	6.38	5.93	5.38	5.70	—
75	6.20	5.71	5.30	10.27	7.67	6.91	6.43	5.82	5.76	—
82	6.49	5.94	5.38	10.60	8.18	7.38	6.87	6.22	5.64	—
90	6.60	6.02	5.35	10.86	8.58	7.75	7.22	6.54	5.49	—
97	6.53	5.91	5.16	10.99	8.86	8.01	7.46	6.77	5.42	—
105	6.31	5.66	4.80	10.96	9.03	8.16	7.61	6.92	5.48	—
112	6.06	5.35	4.33	10.80	9.18	8.28	7.71	7.03	5.62	—
120	5.91	5.10	3.85	10.60	9.39	8.47	7.88	7.17	5.80	—
127	5.99	5.06	3.50	10.46	9.81	8.85	8.23	7.47	5.98	—
135	6.40	5.31	3.38	10.51	10.52	9.52	8.85	8.03	6.23	—
142	7.14	5.87	3.55	10.80	11.54	10.51	9.81	8.90	6.62	—
150	8.13	6.70	3.99	11.32	12.83	11.77	11.02	10.05	7.24	—
157	9.22	7.65	4.58	11.97	14.20	13.13	12.36	11.34	8.05	—
165	10.02	8.53	5.18	12.63	15.44	14.37	13.58	12.53	8.90	—
172	10.89	9.15	5.63	13.10	16.30	15.23	14.44	13.39	9.56	—
180	11.14	9.38	5.79	13.28	16.61	15.54	14.75	13.70	9.81	—

curvature matrix (1%). In tables 4 and 5 we also detail, at selected scattering angles, the results of the present theoretical calculations for both states although only for the energies investigated in the experiments.

For the purpose of the present discussion we consider each electronic state in turn. Furthermore, because of the quite extensive set of energies studied in this report only representative figures are included in the manuscript. At 5, 6, 15 and 20 eV, i.e. in the regions away from the effects of the $^2\Pi_u$ resonance (Middleton *et al* 1992), we would characterize the level of agreement between the present data and calculation for the a $^1\Delta_g$ state as being very good. This is indicated by figures 4(*a*) and 4(*b*) which show the differential cross sections for the a $^1\Delta_g$ state at $E_0 = 6$ eV and 15 eV, respectively. Within the combined uncertainties on the various data sets the present measurement and that of Trajmar *et al* (1971), Wong *et al* (1973) and Shyn and Sweeney (1993) are also found to be in fair agreement at all of the common energies in the above range. In particular we highlight the very good agreement between the present experimental data and that of Shyn and Sweeney (1993) at $E_0 = 10$ eV. At 20 eV we can also compare the present data with the experiment of Wakiya (1978a, b). Here we find that their data is in better agreement, in terms of the absolute magnitude of the differential cross sections, with the current data than with the earlier work of Trajmar *et al* (1971) although within the combined uncertainties of the various measurements the overall level of agreement is fair. In terms of the shapes of the respective differential cross

Table 5. Theoretical differential cross sections (10^{-19} cm^2 sr^{-1}) for electron impact excitation of the b $^1\Sigma_g^+$ electronic state.

Scattering angle θ_e (deg)	$\sigma(\theta)$ Incident electron beam energy (eV)									
	5.0	6.0	7.0	8.0	9.0	9.5	10.0	11.0	15.0	20.0
0	0.00	0.00	0.00	0.00	0.00	0.00	0.00	0.00	0.00	—
6	0.07	0.06	0.04	0.10	0.12	0.11	0.10	0.09	0.07	—
14	0.38	0.32	0.18	0.52	0.62	0.57	0.53	0.48	0.34	—
22	0.85	0.71	0.40	1.21	1.42	1.30	1.21	1.08	0.76	—
30	1.39	1.15	0.63	2.07	2.35	2.14	1.98	1.76	1.20	—
36	1.77	1.45	0.79	2.76	3.03	2.74	2.53	2.24	1.50	—
44	2.16	1.76	0.95	3.66	3.82	3.42	3.14	2.76	1.79	—
52	2.39	1.93	1.07	4.48	4.36	3.86	3.52	3.07	1.96	—
60	2.43	1.96	1.16	5.20	4.62	4.04	3.66	3.17	2.02	—
66	2.38	1.93	1.25	5.66	4.63	4.02	3.63	3.12	2.01	—
74	2.24	1.86	1.42	6.17	4.46	3.82	3.43	2.94	1.95	—
82	2.08	1.80	1.77	6.55	4.13	3.49	3.11	2.68	1.85	—
90	1.98	1.81	2.04	6.79	3.70	3.09	2.75	2.37	1.72	—
96	1.94	1.87	2.33	6.86	3.36	2.78	2.47	2.14	1.61	—
104	1.95	1.97	2.69	6.77	2.89	2.37	2.11	1.84	1.45	—
112	1.98	2.08	2.96	6.46	2.44	1.99	1.78	1.57	1.28	—
120	1.98	2.11	3.06	5.90	2.02	1.64	1.47	1.32	1.11	—
126	1.92	2.06	2.98	5.33	1.71	1.40	1.26	1.14	0.98	—
134	1.75	1.87	2.69	4.41	1.33	1.09	0.99	0.90	0.80	—
142	1.44	1.55	2.19	3.36	0.89	0.80	0.73	0.68	0.62	—
150	1.06	1.13	1.58	2.29	0.57	0.54	0.49	0.46	0.43	—
156	0.74	0.79	1.10	1.55	0.43	0.36	0.33	0.31	0.29	—
164	0.36	0.38	0.53	0.73	0.20	0.17	0.16	0.15	0.14	—
172	0.09	0.10	0.14	0.19	0.05	0.04	0.04	0.04	0.04	—
180	0.00	0.00	0.00	0.00	0.00	0.00	0.00	0.00	0.00	—

sections then at 20 eV there is good agreement between ourselves, Wakiya (1978a, b) and Trajmar *et al* (1971).

Middleton *et al* (1992) found that the integral cross section for the resonance enhanced a $^1\Delta_g$ state excitation peaked at about 10 eV whilst Noble and Burke (1992) found this same peak to be at 8 eV. This discrepancy in the position of the maximum of the integral cross section is also reflected in the level of agreement between the present theoretical and experimental differential cross sections in the resonance region, i.e. $E_0 \sim 7$–11 eV. In this energy regime the general trend in the level of agreement is most easily assessed by comparing differential cross sections for fixed angles as a function of the scattering energy. The differential cross sections corresponding to scattering angles of 30°, 60° and 90° are illustrated in figures 5(*a*)-(*c*), respectively. These figures demonstrate that despite the discrepancy between theory and experiment concerning the position of the peak in the cross section there is otherwise good agreement on the overall trends and on the general magnitude of the cross section. With the exception of 7 eV, the differential cross section measurements of Wong *et al* (1973) at $\theta_e = 25°$ are in excellent agreement with the present data over the entire energy range 7–11 eV. Both Trajmar *et al* (1971) and Shyn and Sweeney (1993) only reported data at 7 and 10 eV in the energy region we are now discussing. At 10 eV the data of Trajmar *et al* (1971) is in poor agreement with both the current experiment and theory and the recent

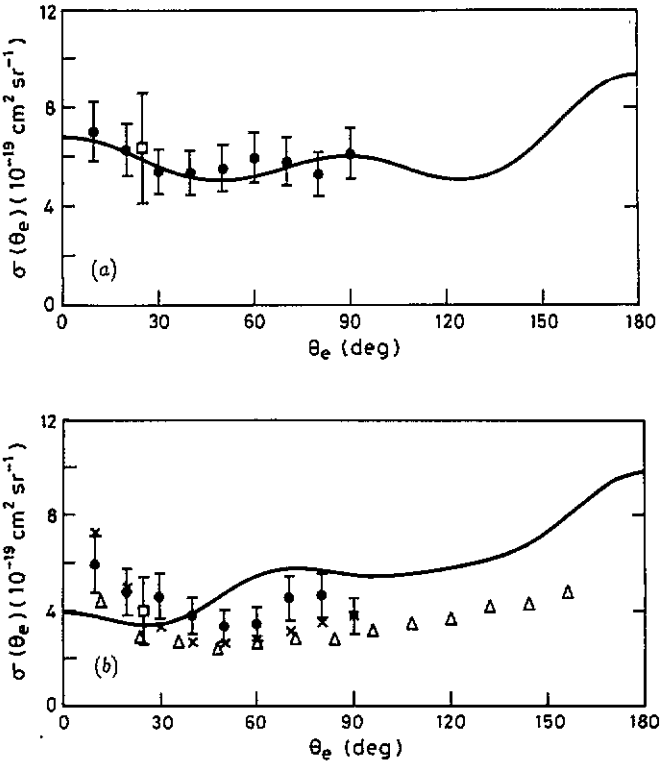

Figure 4. Differential cross sections for electron impact excitation of the a $^1\Delta_g$ state of O_2. (*a*) $E_0 = 6$ eV, (*b*) $E_0 = 15$ eV. The present data (●) and theory (——), are compared with the earlier work of Wong *et al* (1973) (□), Shyn and Sweeney (1993) (△) and Trajmar *et al* (1971) (×).

experiment of Shyn and Sweeney although at 7 eV the agreement of Trajmar *et al's* data with the present calculation is fair.

Middleton *et al* (1992) have previously noted that the inclusion of nuclear motion into the *R*-matrix calculation of Noble and Burke (1992) could well lead to better agreement between experiment and theory with respect to the position of Q_{max}. The energies of the target states around 6 eV, which are associated with the Feshbach resonance, are seen from table 1 to be of limited accuracy and could also be the source of error within the calculation. In either case it is possible that the level of agreement between experiment and theory for the differential cross section for the excitation of the a $^1\Delta_g$ state would also improve in the 7–11 eV electron beam energy range.

The level of agreement between the present experiment and calculation for the electronic excitation of the b $^1\Sigma_g^+$ state is also good. The form of this cross section is largely determined by the 'selection rule' discussed by Cartwright *et al* (1971). They showed that for $\Sigma^+ \rightarrow \Sigma^-$ transitions there are symmetry constraints which imply that the differential cross section $\sigma(\theta)$ should tend to zero when the scattering angle θ_e approaches 0° or 180°. Indeed the present experiment and that of Trajmar *et al* (1971) are both consistent at forward angles with this expectation. With the exception of the data at 10 eV, our experimental measurement and that of Trajmar *et al* (1971) are in good agreement, at the common energies of both studies, in terms of both the shapes and magnitudes of the differential cross sections. The recent measurement of Shyn and

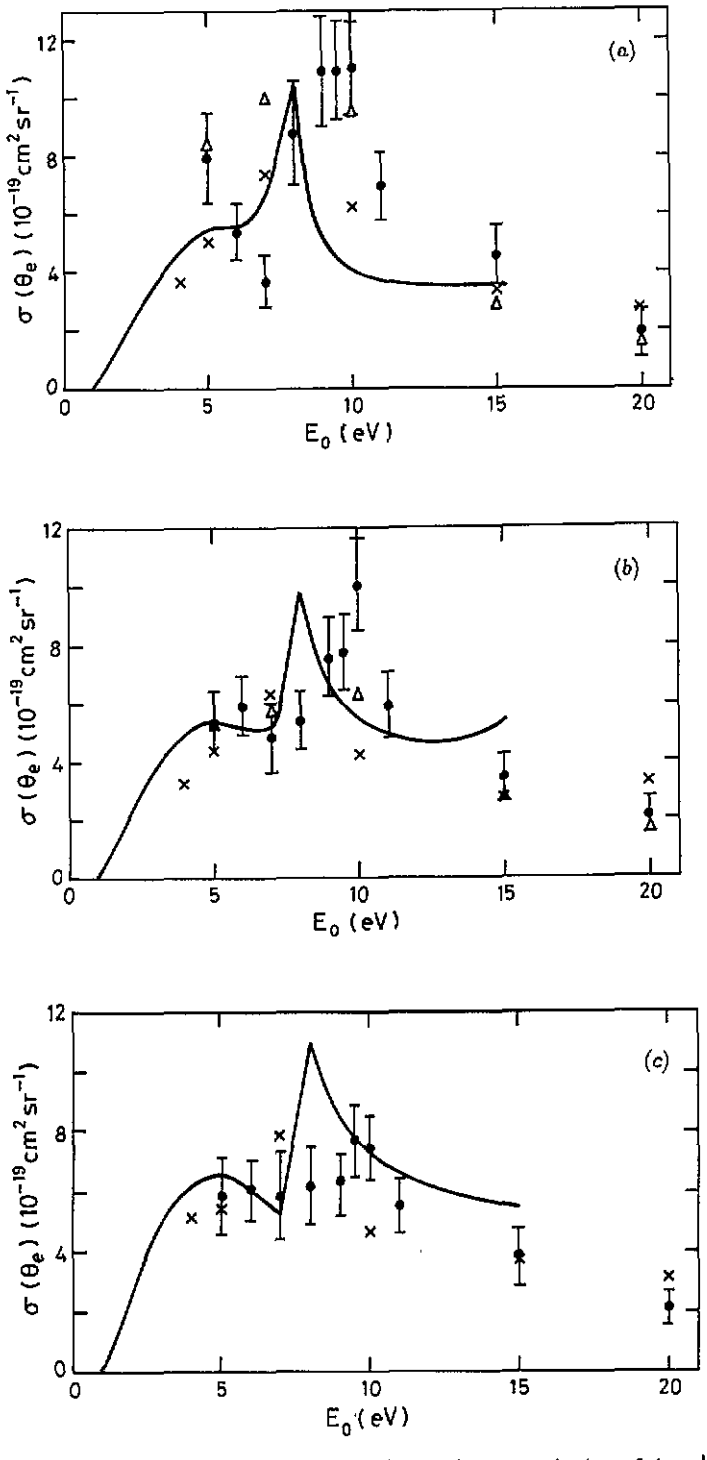

Figure 5. Differential cross sections for electron impact excitation of the a $^1\Delta_g$ state of O_2 plotted as a function of the scattering energy E_0 for fixed scattering angles. (*a*) $\theta_e = 30°$, (*b*) $\theta_e = 60°$, (*c*) $\theta_e = 90°$. The present data (●) and theory (——) are compared with the earlier work of Wong *et al* (1973) (□), Shyn and Sweeney (1993) (△) and Trajmar *et al* (1971) (×).

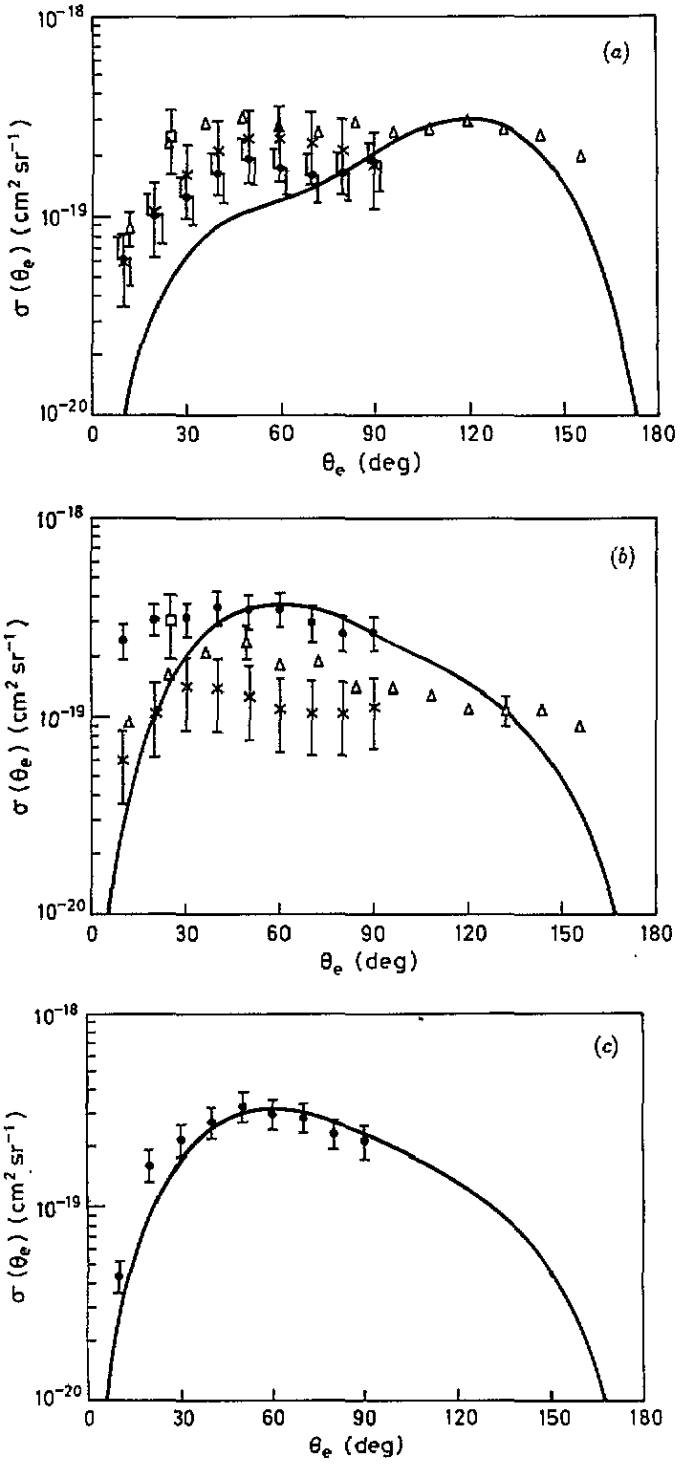

Figure 6. Differential cross sections for electron impact excitation of the b $^1\Sigma_g^+$ state of O_2. (*a*) $E_0 = 7$ eV, (*b*) $E_0 = 10$ eV, (*c*) $E_0 = 11$ eV, (*d*) $E_0 = 15$ eV. The present data (●) and theory (——) are compared with the earlier work of Wong *et al* (1973) (□), Shyn and Sweeney (1993) (△) and Trajmar *et al* (1971) (×).

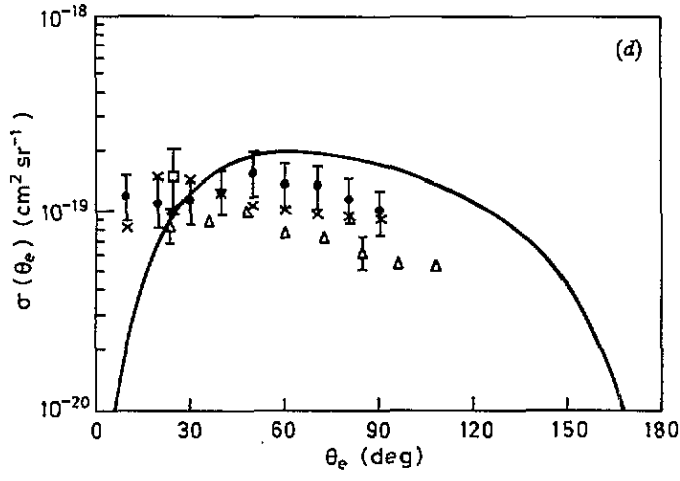

Figure 6. (continued)

Sweeney (1993) at 10 eV is in better agreement with the present data than that of the work of Trajmar *et al* (1971) although it too underestimates the magnitude of the b $^1\Sigma_g^+$ cross section to some extent. In general though we would characterize the level of agreement between the present data and Shyn and Sweeney (1993) as being fair for the common energies 7, 10, 15 and 20 eV. The data of Wong *et al* (1973) at $\theta_e = 25°$ is also found to be in good agreement with the current experimental data over the entire energy regime of interest. Similarly, the work of Wakiya (1978a, b) at 20 eV is in fair agreement with both ourselves and Trajmar *et al* (1971). Consequently we conclude that there exists a body of experimental differential cross section data for the b $^1\Sigma_g^+$ state which are by and large in pretty good agreement with each other.

The largest discrepancy between the present experiment and the *R*-matrix calculations occurs at a scattering energy of 6 eV as can be seen in the tables. At this energy the measured cross sections show a deep dip with a minimum at $\theta_e = 60°$ whereas theory shows a shallow minimum at a scattering angle of 90°. We also note, with the exception of figure 6(*c*) where the agreement between the present experiment and theory is good across the entire angular range, a small but not insignificant discrepancy at the very forward angles. We believe that this is likely to be due to a combination of the fact that the present calculation does not account for all polarization effects and that the measured experimental data have associated with them a finite angular resolution effect. The latter effect is only important when the cross section varies rapidly as a function of angle, which is indeed the case as $\theta_e \rightarrow 0°$ for the b $^1\Sigma_g^+$ state. There is good agreement between theory and the measurements of Trajmar *et al* (1971) at a scattering energy of 4 eV and with the present experiment at other energies. The level of agreement is illustrated in figures 6(*a*)–(*d*) which compare measured and calculated differential cross sections at energies of 7, 10, 11 and 15 eV respectively. For this transition the agreement between theory and experiment is most clearly illustrated by plotting differential cross sections for fixed scattering energies as a function of the scattering angle. In general there is marginally closer agreement between theory and the present measurements than with previous measurements.

The results presented demonstrate a reasonably satisfactory agreement between theory and experiment for both of the transitions considered apart from the location

of the $^2\Pi_u$ resonance. The remaining discrepancies can almost certainly be accounted for by the use of relatively simple target descriptions (and to a lesser extent the neglect of nuclear motion effects) in the theoretical calculations. More efficient algorithms are being developed to enable more accurate target wavefunctions to be used in scattering calculations. Detailed studies of these effects will be reported in a later publication.

Acknowledgments

Two of us (CJN, PGB) wish to thank the SERC for support under a rolling grant. The experimental work in this manuscript was supported in part from a grant by the Australian Research Council (ARC). MJB acknowledges the ARC for the financial support of a Fellowship.

References

Badger R M, Wright A C and Whitlock R F 1965 *J. Chem. Phys.* **43** 4345
Beebe N H F, Thulstrup E W and Andersen A 1976 *J. Chem. Phys.* **64** 2080
Brunger M J and Teubner P J O 1990 *Phys. Rev.* A **41** 1413–26
Brunger M J, Teubner P J O, Weigold A M and Buckman S J 1989 *J. Phys. B: At. Mol. Opt. Phys.* **22** 1443–53
Buenker R J and Peyerimhoff S 1975 *Chem. Phys. Lett.* **34** 225
Burke V M and Noble C J 1994 to be published
Cartwright D C, Chutjian A, Trajmar S and Williams W 1977 *Phys. Rev.* A **16** 1013–40
Cartwright D C, Trajmar S, Williams W and Huestis D L 1971 *Phys. Rev. Lett.* **27** 704–7
Dill D and Dehmer J L 1974 *J. Chem. Phys.* **61** 692–9
Fano U and Dill D 1972 *Phys. Rev.* A **6** 185
Gauyacq J P, Teillet-Billy D, Malegat L, Abouaf R and Benoit C 1987 *Proc. 15th Int. Conf. on Physics of Electronic and Atomic Collisions (Brighton)* (Amsterdam: North-Holland) Abstracts p 313
Gillan C J, Nagy O, Burke P G, Morgan L A and Noble C J 1987 *J. Phys. B: At. Mol. Phys.* **20** 4585
Huber K P and Herzberg G 1979 *Constants of Diatomic Molecules* (New York: Van Nostrand Reinhold)
Khakoo M A, Newell W R and Smith A C H 1983 *J. Phys. B: At. Mol. Phys.* **16** L317
Konishi A, Wakiya K, Yamamoto M and Suzuki H 1970 *J. Phys. Soc. Japan* **29** 526–8
Krupenie P H 1972 *J. Phys. Chem. Ref. Data* **1** 423
Linder F and Schmidt H 1971 *Z. Naturf.* **26** 1617–25
McDermott W E, Pchelkin N R, Bernard D J and Bouseh R R 1978 *Appl. Phys. Lett.* **32** 469
Middleton A G, Teubner P J O and Brunger M J 1992 *Phys. Rev. Lett.* **69** 2495
Nesbet R K 1979 *Phys. Rev.* A **20** 58–70
Noble C J and Burke P G 1986 *J. Phys. B: At. Mol. Phys.* **19** L35–9
—— 1992 *Phys. Rev. Lett.* **68** 2011–4
Pichou F, Heutz A, Joyez G, Landau M and Mazeau J 1976 *J. Phys. B: At. Mol. Phys.* **9** 933–44
Saxon R P and Liu B 1977 *J. Chem. Phys.* **67** 5432–41
Schulz G J and Dowell J T 1962 *Phys. Rev.* **128** 174–7
Skerbele A, Dillon M A and Lassettre E N 1968 *J. Chem. Phys.* **49** 3542–5
Shyn T W and Sharp W E 1982 *Phys. Rev.* A **26** 1369–72
Shyn T W and Sweeney C J 1993 *Phys. Rev.* A **47** 1006–8
Teillet-Billy D, Malegat L and Gauyacq J P 1987 *J. Phys. B: At. Mol. Phys.* **20** 3201–16
Trajmar S, Cartwright D C and Williams W 1971 *Phys. Rev.* A **4** 1482–92
Wakiya K 1978a *J. Phys. B: At. Mol. Phys.* **11** 3913–30
—— *J. Phys. B: At. Mol. Phys.* **11** 3931–8
Watson C E, Dulock V A, Stolarski R S and Green A E S 1967 *J. Geophys. Res.* **72** 3961
Wöste G and Fullerton C 1994 to be published
Wong S F, Boness M J W and Schulz G J 1973 *Phys. Rev. Lett.* **31** 969–71